

## Supporting Information

### Large-area grown ultrathin molybdenum oxide for label-free sensitive biomarker detection

Jiaru Zhang,<sup>a</sup> Yange Luan,<sup>a</sup> Qijie Ma,<sup>a</sup> Yihong Hu,<sup>a</sup> Rui Ou,<sup>a</sup> Crispin Szydzik,<sup>a</sup> Yunyi Yang,<sup>b</sup> Vien Trinh,<sup>a</sup> Nam Ha,<sup>a</sup> Zhenyue Zhang,<sup>a</sup> Guanghui Ren,<sup>a</sup> Hu Jun Jia,<sup>c</sup> Bao Yue Zhang<sup>\*a,d</sup>, and Jian Zhen Ou<sup>\*a</sup>

<sup>a</sup>School of Engineering, RMIT University, Melbourne 3000, Australia

<sup>b</sup>School of Science, Computing and Engineering Technologies, Swinburne University of Technology, Hawthorn, Victoria 3122, Australia

<sup>c</sup>College of Microelectronics, Xidian University, Xi'an, Shaanxi, 710000, China

<sup>d</sup>School of Physics and Astronomy, Monash University, Clayton, Victoria, 3800 Australia

Corresponding Author

\* Email: baoyue.zhang@rmit.edu.au (B.Y.Z.)

\* Email: jianzhen.ou@rmit.edu.au (J.Z.O.)

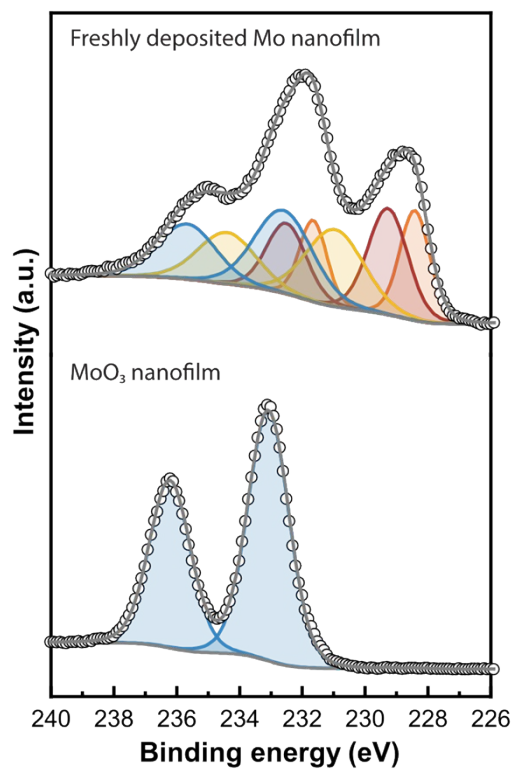


**Figure S1.** The XPS spectra of freshly deposited ultrathin Mo film (top) and MoO<sub>3</sub> nanofilm after oxidation process (bottom). The fitted molybdenum metal peaks (228.4 eV and 231.6 eV), Mo<sup>4+</sup> peaks (229.2 eV and 232.4 eV), Mo<sup>5+</sup> peaks (231.0 eV and 234.2 eV), and Mo<sup>6+</sup> peaks (232.7 eV and 235.8 eV) are indicated in the graph.

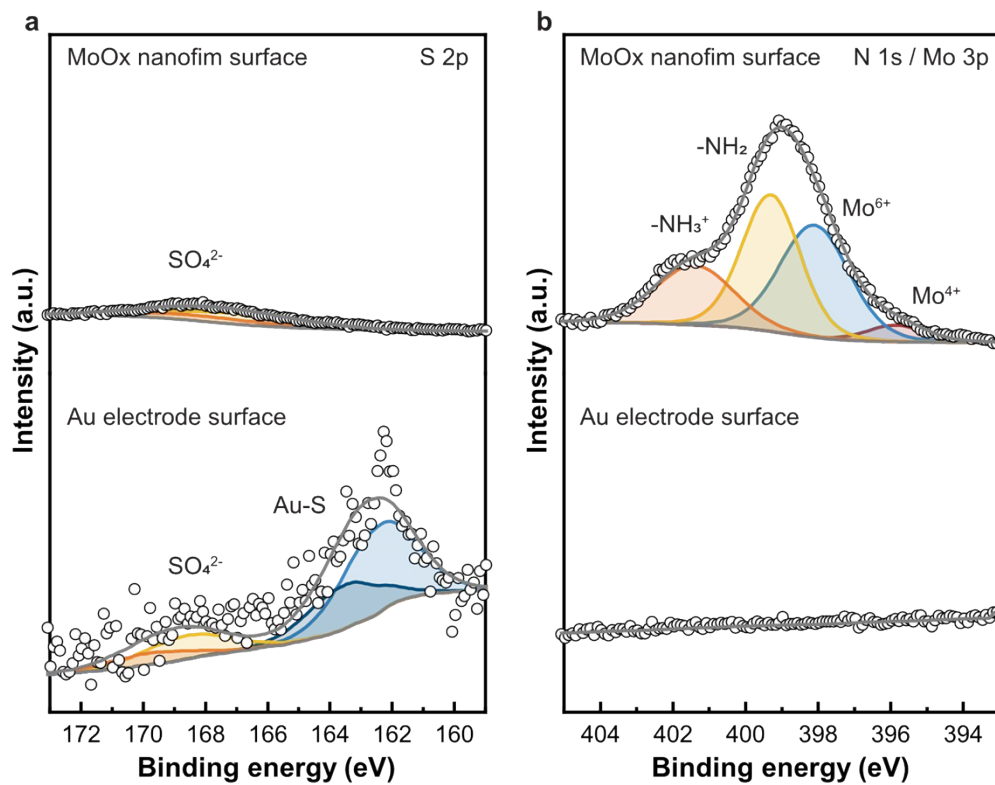


**Figure S2.** Comparison of high resolution XPS spectra of MoO<sub>x</sub> nanofilm surface (top) and Au electrode surface (bottom) after functionalization with APTES for (a) N 1s; (b) S 2p. The low signal-to-noise ratio of S2p is due to the dual factors of sole S atom in each 1-Dodecanethiol molecule<sup>1</sup> and low concentration (10 mM) of 1-Dodecanethiol molecule incubated in ethanol solution [1, 2].

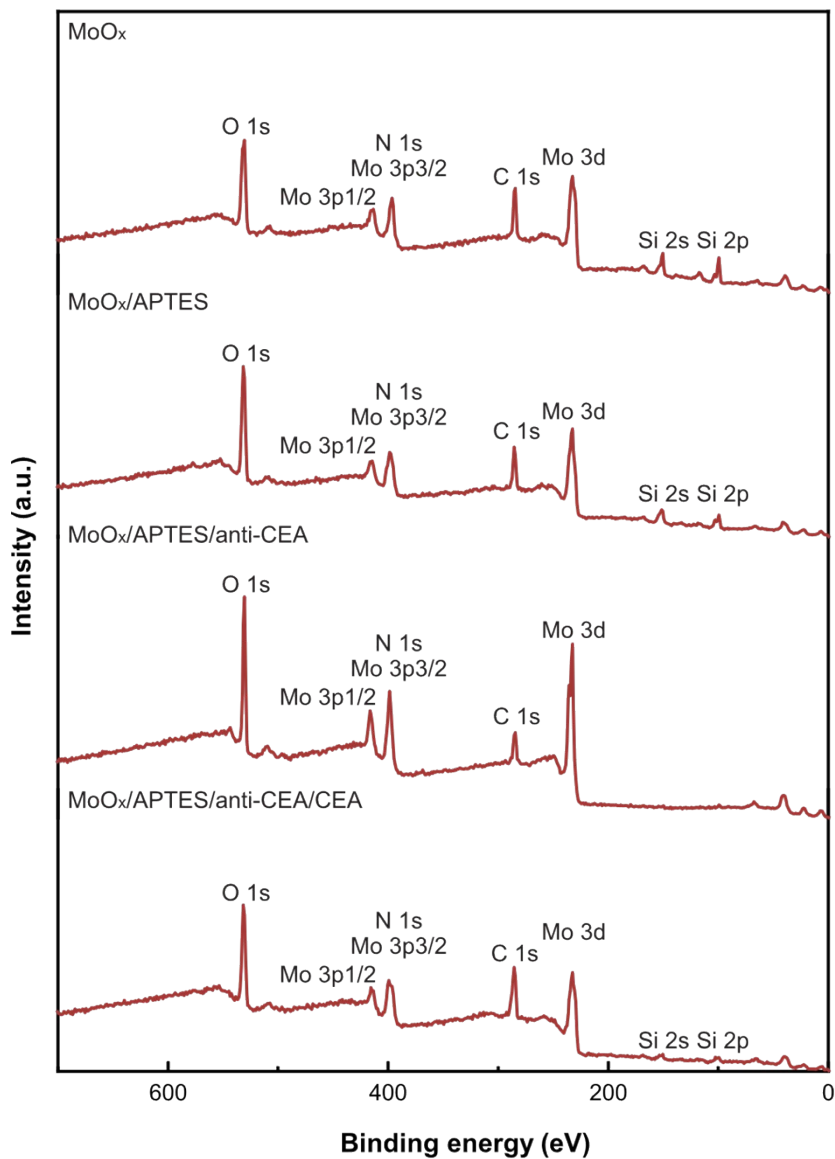


**Figure S3.** XPS survey for MoO<sub>x</sub>, MoO<sub>x</sub>/APTES, MoO<sub>x</sub>/APTES/anti-CEA, and MoO<sub>x</sub>/APTES/anti-CEA/CEA.

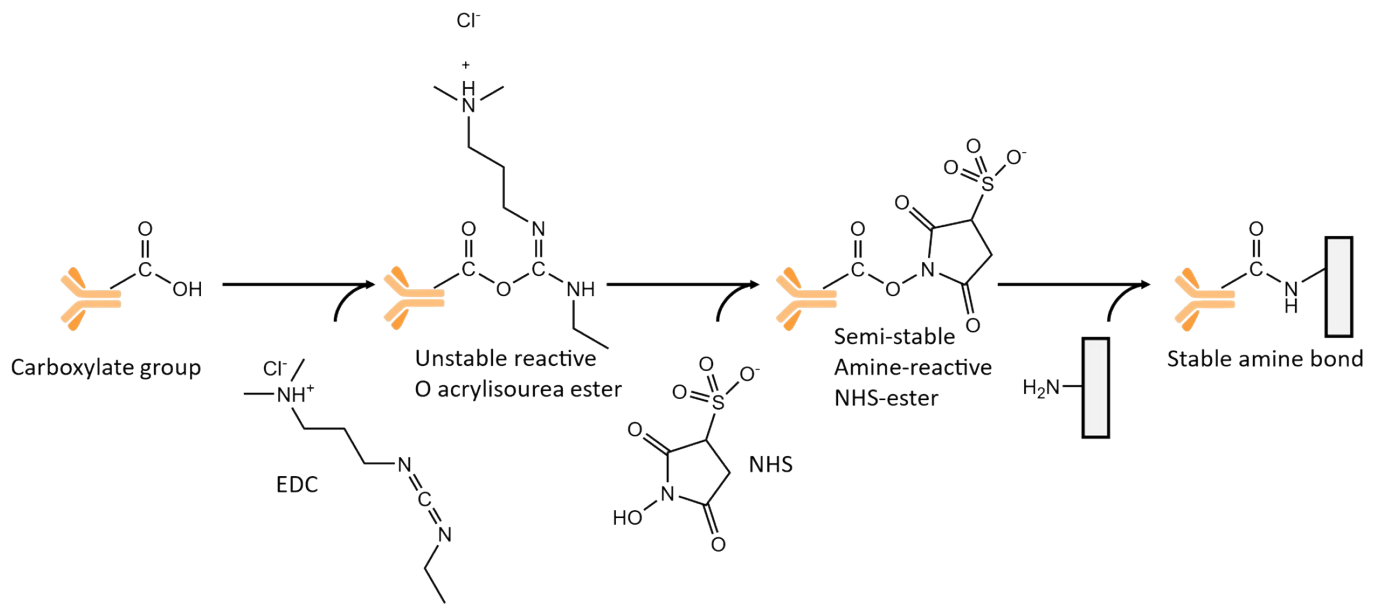


**Figure S4.** Immobilization of anti-CEA on an amine group functionalized surface mediated by EDC and NHS coupling.

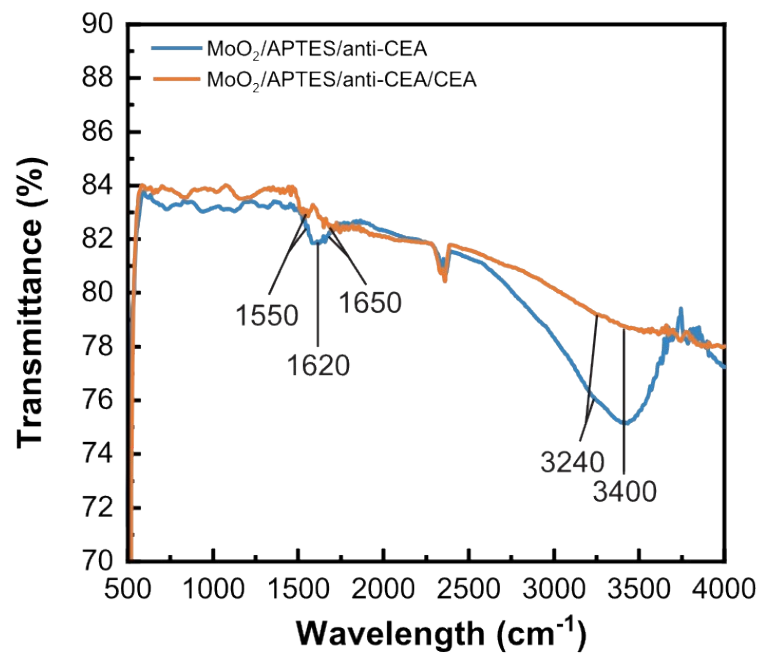
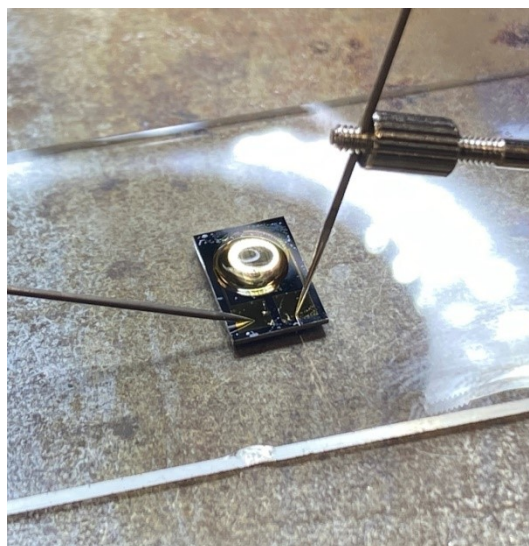


Figure S5. FTIR spectra of MoO<sub>x</sub>/APTES/anti-CEA, and MoO<sub>x</sub>/APTES/anti-CEA/CEA.

**Table S1.** Detailed composition of ultrathin MoO<sub>x</sub> film in different functionalization stage calculated from the XPS

	Ref	MoO <sub>x</sub> /APTES	MoO <sub>x</sub> /APTES/anti-CEA	MoO <sub>x</sub> /APTES/anti-CEA/CEA
Mo <sup>6+</sup> [%]	16.55	25.83	12.94	11.01
Mo <sup>5+</sup> [%]	28.64	21.77	24.55	25.12
Mo <sup>4+</sup> [%]	54.80	52.4	62.52	63.87
x	2.31	2.37	2.25	2.24



**Figure S6.** Electrical measurements on the developed  $\text{MoO}_x$ -IDE biosensing chip with output characteristic at a fixed 0.1 V source voltage.



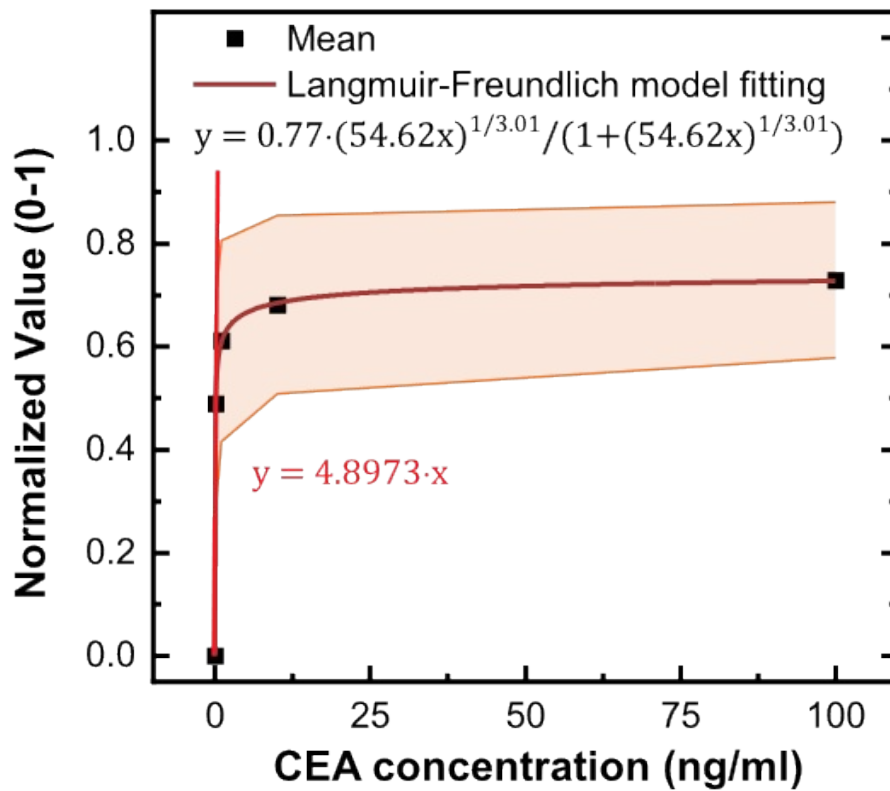


Figure S7. the slope of the linear region of the Langmuir-Freundlich model fitted curve.

**Table S2.** Comparisons of the sensing performance of developed electronic biosensing chip with other methods for the detection of CEA biomarker.

Device	Detection Type	Linear range (ng/ mL)	Detection limit (ng/ mL)	Reference
anti-CEA/ADA-COOH/APTES/SiO <sub>2</sub> /IDE	Labeled	0.1 - 1000	0.007	[3]
Si <sub>3</sub> N <sub>4</sub> /Au/IDE	Label-free	0.0001 - 10	0.0001	[4]
anti-CEA/PRY-NHS/Graphene/FET	Label-free	0.1 - 100	0.1	[5]
anti-CEA/denatured-BSA/Graphene/FET	Labeled	0.01 - 100	0.00034	[6]
anti-CEA/MoS <sub>2</sub> -Au/GCE	Labeled	0.001 - 50	0.00027	[7]
Anti-CEA/APTES/MoO <sub>x</sub> /IDE	Label-free	0.1-100	0.015	This work

## Reference

1. Sigma-Aldrich. "1-Dodecanethiol." <https://www.sigmaaldrich.com/AU/en/product/aldrich/471364> (accessed 04-05, 2024).
2. N. Mahmoodi et al., "Room temperature thermally evaporated thin Au film on Si suitable for application of thiol self-assembled monolayers in micro/nano-electro-mechanical-systems sensors," *Journal of Vacuum Science & Technology A*, vol. 35, no. 4, 2017.
3. Li, X., Yu, M., Chen, Z., Lin, X., and Wu, Q., A sensor for detection of carcinoembryonic antigen based on the polyaniline-Au nanoparticles and gap-based interdigitated electrode. *Sens. Actuators, B*, 2017, 239, 874-882.
4. Jin, Y., Mao, H., Jin, Q., and Zhao, J., Real-time determination of carcinoembryonic antigen by using a contactless electrochemical immunosensor. *Analytical Methods*, 2016, 8(24), 4861-4866.
5. Zhou, L., Mao, H., Wu, C., Tang, L., Wu, Z., Sun, H., Zhang, H., Zhou, H., Jia, C., and Jin, Q., Label-free graphene biosensor targeting cancer molecules based on non-covalent modification. *Biosensors and Bioelectronics*, 2017, 87, 701-707.
6. Zhou, L., Wang, K., Sun, H., Zhao, S., Chen, X., Qian, D., Mao, H., and Zhao, J., Novel graphene biosensor based on the functionalization of multifunctional nano-bovine serum albumin for the highly sensitive detection of cancer biomarkers. *Nano-micro letters*, 2019, 11(1), 1-13.
7. Wang, X., Chu, C., Shen, L., Deng, W., Yan, M., Ge, S., Yu, J., and Song, X., An ultrasensitive electrochemical immunosensor based on the catalytical activity of MoS<sub>2</sub>-Au composite using Ag nanospheres as labels. *Sens. Actuators, B*, 2015, 206, 30-36.